Biosensors and Bioelectronics 137 (2019) 148–153

Contents lists available at ScienceDirect

Biosensors and Bioelectronics

journal homepage: www.elsevier.com/locate/bios

A ratiometric fluorescent assay for the detection and bioimaging of alkaline phosphatase based on near infrared Ag_2S quantum dots and calcein

Meifang Cai, Caiping Ding, Fangfang Wang, Mingqiang Ye, Cuiling Zhang**, Yuezhong Xian*

Shanghai Key Laboratory of Green Chemistry and Chemical Processes, Department of Chemistry, School of Chemistry and Molecular Engineering, East China Normal University, Shanghai, 200241, China

ARTICLE INFO

Keywords:
Ratiometric detection
Alkaline phosphatase
Near infrared fluorescence probe
Quantum dots
Calcein

ABSTRACT

Herein, a ratiometric fluorescent method was developed for alkaline phosphatase (ALP) detection based on near-infrared (NIR) Ag_2S quantum dots (QDs) and calcein through the competitive approach. The system based on Ag_2S QDs and calcein shows green (maximum emission at 512 nm from calcein) and near infrared (NIR) fluorescence (maximum 798 nm from Ag_2S QDs) under the same excitation wavelength (468 nm). In the presence of Ce^{3+}, the fluorescence intensity of calcein is decreased due to static quenching, while the fluorescence intensity of Ag_2S QDs is enhanced through aggregation induced emission (AIE). The p-nitrophenyl phosphate is hydrolyzed by ALP, and the yield phosphate ions bind with Ce^{3+} with higher affinity than these of Ag_2S QDs and calcein. Therefore, the green fluorescence from calcein is recovered while NIR fluorescence from Ag_2S QDs is decreased. On the basis of these findings, a ratiometric fluorescence assay was developed for the measurement of ALP activity. The ratio of fluorescence intensity at 512 and 798 nm (F_{512}/F_{798}) was well associated with the ALP concentration ranging from 2 to 100 mU/mL with the detection limit of 1.28 mU/mL. The method was successfully applied for detecting ALP in human serum with an acceptable recovery and bioimaging intracellular ALP with good performance. In addition, the approach was also employed for the screening ALP inhibitor.

1. Introduction

As one of the essential phosphate group hydrolases, alkaline phosphatase (ALP) is widely presented in biological system, which can catalyze hydrolysis of phosphate ester groups of various substrates, such as small molecules, proteins and nucleic acids (Coleman, 1992; Harris, 1990; Alonso et al., 2004; Lallès, 2014). ALP plays critical roles in many physiological processes, such as signal transmission, cell growth and apoptosis (Julien et al., 2011; Choi et al., 2007). The abnormal level of ALP in serum is tightly related to many diseases, such as bone disease (Couttenye et al., 1996), liver dysfunction (Colombatto et al., 1996; Ooi et al., 2007) and prostate cancer (Lorente et al., 1999). Moreover, as a kind of secreted proteins, the bioactivity of ALP also indicates the state of local cells. The real-time monitoring of ALP in cells can distinguish normal and abnormal behavior of cells (Arai et al., 2013). Therefore, it is of great significance to develop a sensitive, selective and reliable method for detecting ALP activity in biological system.

So far, a number of methods have been developed for ALP detection, including electrochemistry (Ino et al., 2012; Goggins et al., 2015), colorimetry (Jiao et al., 2014; Deng et al., 2013), fluorometry (Qian et al., 2015a; Ma et al., 2016), chemiluminescence (Blum et al., 2001) and surface-enhanced Raman scattering (Ruan et al., 2006). Among them, the fluorescent method is extremely attractive because of its easy operation, high sensitivity, noninvasive and real-time monitoring in living cells and organisms (Lu et al., 2016a; Deng et al., 2011; Li et al., 2014; Hu et al., 2014). However, many fluorescent methods for ALP detection are performed using ultraviolet or visible light as excitation source, which limits their applications in bioimaging (Tong et al., 2018; Xiang et al., 2016). Recently, some near-infrared (NIR) organic probes were developed for the bioimaging of endogenous ALP in living cells. For example, Lee's group developed two organic dye-based NIR probes with a phenolic dihydroxanthene fluorophore core and a phosphate with sulfonate group for the imaging of endogenous ALP in HeLa, HepG2 and MC3T3-E1 cells (Park et al., 2018). Li et al. reported a NIR fluorescent probe based on hemicyanine dye for highly sensitive detection and imaging of ALP in HeLa cells (Li et al., 2017). Wang's group demonstrated a dicyano-based ratiometric fluorescent probe for ALP sensing in HeLa cells (Lu et al., 2016b). However, organic fluorophores usually suffer from poor water solubility, underlying photobleaching

* Corresponding author.
** Corresponding author.
E-mail addresses: clzhang@chem.ecnu.edu.cn (C. Zhang), yzxian@chem.ecnu.edu.cn (Y. Xian).

https://doi.org/10.1016/j.bios.2019.04.057
Received 12 January 2019; Received in revised form 3 April 2019; Accepted 29 April 2019
Available online 07 May 2019
0956-5663/

and complex synthesis procedures. Furthermore, dual-signal readout analytical strategy has attracted great attention, because it can decrease the interference from the complex matrix and improve the sensitivity (Dai et al., 2015; Shi et al., 2012; Fan et al., 2016). To the best of our knowledge, few ratiometric fluorescent probes with the NIR fluorescence emission have been reported for ALP sensing and imaging in living cells.

Taking the advantages of excellent NIR emission, biocompatibility and photostability, Ag_2S quantum dots (QDs) are attractive for applications in biosensing and bioimaging (Gui et al., 2014; Jin et al., 2017). Our previous work indicated that the fluorescence intensity of 3-mercaptopropionic acid (3-MPA) stabilized Ag_2S QDs (3-MPA-Ag_2S QDs) could be enhanced by rare earth ions *via* aggregation-induced emission (AIE) (Ding et al., 2017). Calcein, as a cheap and commercial dye, can emit stable yellow-green fluorescence and is often used as a targeting dye for the cytoplasm (Cheng et al., 2018). The fluorescence of calcein can be efficiently quenched by Ce^{3+} (Berregi et al., 1999; Tomita et al., 2008). Herein, we developed a simple, ratiometric fluorescent method for ALP detection and bioimaging in HeLa cells based on the simple combination of NIR 3-MPA-Ag_2S QDs and calcein. The biosensing system shows a single-excitation and dual emission fluorescence property. As shown in Scheme 1, 3-MPA-Ag_2S QDs and calcein can be simultaneously excited at 468 nm, and emit red emission at 798 nm and green light at 512 nm, respectively. When Ce^{3+} ions are existed in the system, they can bind with carboxyl groups in calcein and 3-MPA-Ag_2S QDs. The fluorescence intensity of 3-MPA-Ag_2S QDs at 798 nm is enhanced while the fluorescence of calcein at 512 nm is quenched. The phosphate ions (PO_4^{3-}) from the direct hydrolysis of p-nitrophenyl phosphate (pNPP) by ALP show higher affinity toward Ce^{3+} ions than these of 3-MPA-Ag2S QDs and calcein. It causes fluorescence recovery of calcein and fluorescence reduction of 3-MPA-Ag_2S QDs. Therefore, the ratio of fluorescence intensity between 3-MPA-Ag_2S QDs and calcein (F_{512}/F_{798}) can be developed for sensitive and selective detection of ALP. The ratiometric fluorescent strategy has been successfully applied for ALP inhibitor screening, ALP detection in human serum and bioimaging in HeLa cells.

2. Experimental section

Details on experimental section were provided in the Supplementary Information.

3. Results and discussion

3.1. Characterization of 3-MPA-Ag_2S QDs and calcein

The image of TEM (Fig. 1A) shows that 3-MPA-Ag_2S QDs have uniform spherical shape, and the average particle size is about 2.6 nm (from the statistics of 250 particles). In addition, the hydrodynamic diameter of the 3-MPA-Ag_2S QDs is about 4.2 nm by DLS (Fig. S1), which is larger than the size observed by TEM due to the presence of the thin ligand coating (3-MPA) on the surface of QDs (Hocaoglu et al., 2012). FTIR spectrum of 3-MPA-Ag_2S QDs in Fig. 1B shows two apparent peaks at 1563 and 1413 cm^{-1}, which are attributed to the asymmetric and symmetric stretching vibration of carboxylate (Hocaoglu et al., 2012). It proves the existence of –COOH on the surface of Ag_2S QDs. Fig. 1C shows the excitation spectra of 3-MPA-Ag_2S QDs and calcein, indicating that the optimum excitation wavelength of 3-MPA-Ag_2S QDs is at 468 nm and the calcein is at 492 nm. Given that the relatively low quantum yield of 3-MPA-Ag_2S QDs, the excitation wavelength of the sensing system is selected as 468 nm for the following experiments. It can be observed that 3-MPA-Ag_2S QDs and calcein are simultaneously excited at 468 nm, and the corresponding maximum emission is obtained at 798 and 512 nm, respectively (Fig. 1D).

3.2. The stability of the ratiometric fluorescence sensing system

The stability of the ratiometric sensing system is further assessed because of the importance for the real applications. As shown in Fig. S2A (line a and b), the fluorescence intensity of 3-MPA-Ag_2S QDs keeps constant after the addition of calcein. The UV–Vis absorption spectrum of calcein does not have any changes in the presence of 3-MPA-Ag_2S QDs (Fig. S2B), suggesting the stability of the system. Moreover, the zeta potentials of 3-MPA-Ag_2S QDs and calcein are negatively charged (Fig. S2C), indicating that no interaction occurs to form a new complex or composite. In addition, Fig. S2D exhibits the excellent photostability

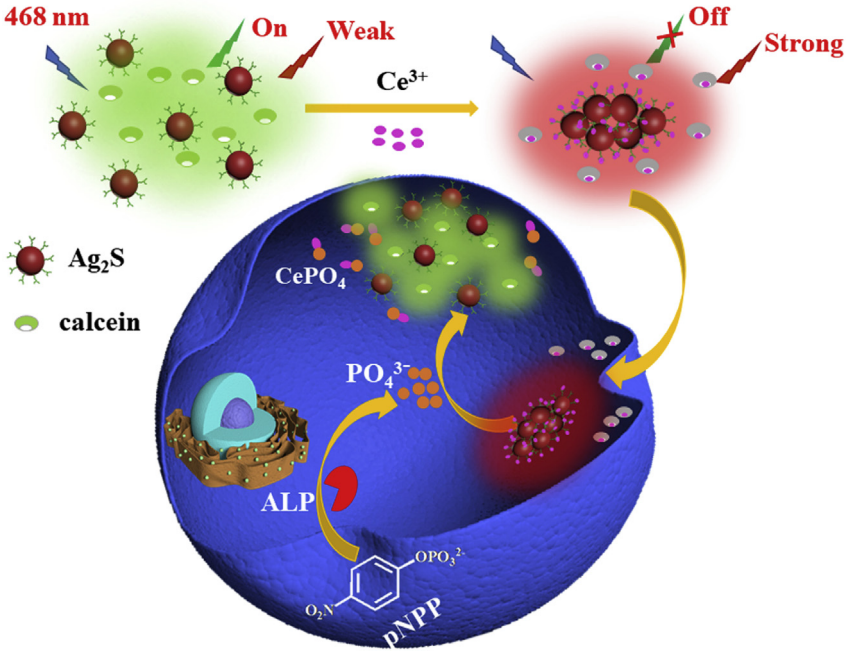

Scheme 1. Schematic representation of the ratiometric fluorescent strategy for ALP detection based on NIR Ag_2S QDs and calcein.

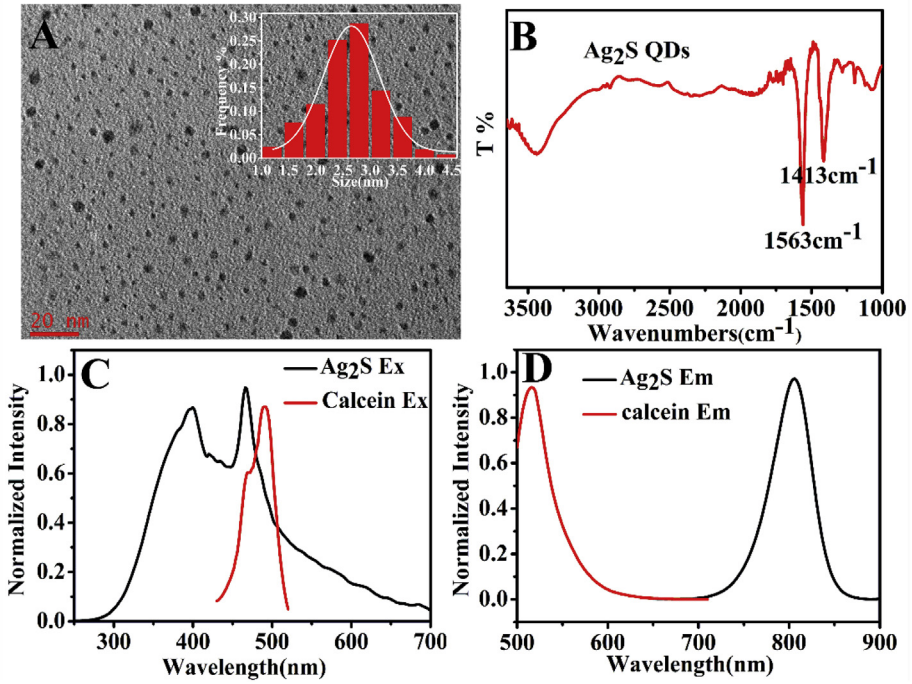

Fig. 1. (A) TEM image of 3-MPA-Ag_2S QDs and inset is the corresponding size distribution; (B) FTIR spectrum for 3-MPA-Ag_2S QDs; (C) the excitation spectra for 3-MPA-Ag_2S QDs and calcein; (D) the emission fluorescence spectra of 3-MPA-Ag_2S QDs and calcein with the excitation wavelength of 468 nm. The concentrations of 3-MPA-Ag_2S QDs and calcein in Fig. 1C and D are 10 μg/ml and 2 nM, respectively.

of the sensing system within 4 h. The fluorescent intensities for 3-MPA-Ag_2S QDs and calcein remain relatively stable over the range of pH 7.0–8.0 (Fig. S2E), which is beneficial for its application in biological system. The effect of ionic strength on the fluorescent intensity is also investigated (Fig. S2F), and the results show negligible influence on 3-MPA-Ag_2S QDs and calcein. All of the results illustrate the good stability of the sensing system based on 3-MPA-Ag_2S QDs and calcein.

3.3. Feasibility for ALP detection

The feasibility of ratiometric fluorescence assay is also investigated. Line a in Fig. 2A is the fluorescence spectrum of the system of 3-MPA-Ag_2S QDs and calcein excited at 468 nm. With the addition of Ce^{3+}, the fluorescence intensity at 512 nm is dramatically reduced while the fluorescence intensity at 798 nm is greatly enhanced (line b in Fig. 2 A). The addition of pNPP or ALP into the system cannot induce obvious changes of the fluorescence intensity (line c and d in Fig. 2A). While ALP and pNPP are simultaneously added, the effect of Ce^{3+} on the fluorescence intensity is decreased (line e in Fig. 2A). While pNPP and ALP are added into the solution containing Ag_2S QDs and calcein without Ce^{3+}, no obvious change of fluorescent intensity is observed (line f in Fig. 2 A). These results indicate that the sensing strategy is suitable for ALP detection.

The mechanism of fluorescence assay is further evaluated. We reported that rare earth ions can enhance the fluorescence of 3-MPA-Ag_2S QDs through AIE (Ding et al., 2017). Therefore, we infer that the mechanism of Ce^{3+}-induced enhancement the fluorescence of 3-MPA-Ag_2S QDs is also attributed to the AIE. The zeta potential for 3-MPA-Ag_2S QDs is about −48.8 mV due to the existence of –COOH. With the addition of Ce^{3+}, the zeta potential is up to −25.7 mV due to the complexation of Ce^{3+} with –COOH (Fig. S3). The TEM image of 3-MPA-Ag_2S QDs with Ce^{3+} is shown in Fig. S4. It can be seen that the particle size is much larger than that of 3-MPA-Ag_2S QDs, indicating Ce^{3+}-induced the aggregation of 3-MPA-Ag_2S QDs. Moreover, the fluorescence lifetime of 3-MPA-Ag_2S QDs is increased from 13.2 to 24.1 ns in presence of Ce^{3+} (line a and c in Fig. 2B). It has been reported that AIE can prolong the fluorescence lifetime of QDs (Ao et al., 2018; Jia et al., 2013). Based on the aforementioned results, we can draw a conclusion that the enhancement of fluorescence at 798 nm is originated from Ce^{3+}-induced AIE of Ag_2S QDs. The fluorescence lifetime of calcein remains stable before (4.1 ns) and after addition of Ce^{3+} (4.0 ns), indicating static quenching mechanism (Fig. 2C). These phenomena have been attributed to competitive affiliations of phosphate ions to Ce^{3+} against 3-MPA- Ag_2S QDs and calcein in the ratiometric sensing system.

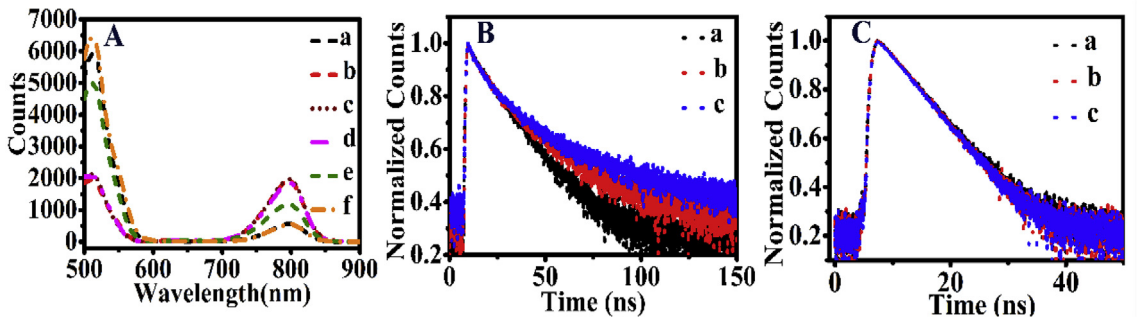

Fig. 2. (A) Fluorescence spectra of 3-MPA-Ag_2S QDs and calcein in presence of different substances. (a) none, (b) Ce^{3+} (100 μM), (c) Ce^{3+} (100 μM) + pNPP (100 μM), (d) Ce^{3+} (100 μM) + ALP (120 mU/mL), (e) Ce^{3+} (100 μM) + pNPP (100 μM) + ALP (120 mU/mL), (f) pNPP (100 μM) + ALP (120 mU/mL); (B) Fluorescence lifetimes of 3-MPA-Ag_2S QDs in presence of (a) calcein, (b) Ce^{3+} (100 μM), pNPP (100 μM) and ALP (120 mU/mL), (c) Ce^{3+} (100 μM); (C) Fluorescence lifetimes of calcein in presence of (a) 3-MPA-Ag_2S QDs, (b) Ce^{3+} (100 μM), pNPP (100 μM) and ALP (120 mU/mL), (c) Ce^{3+} (100 μM).

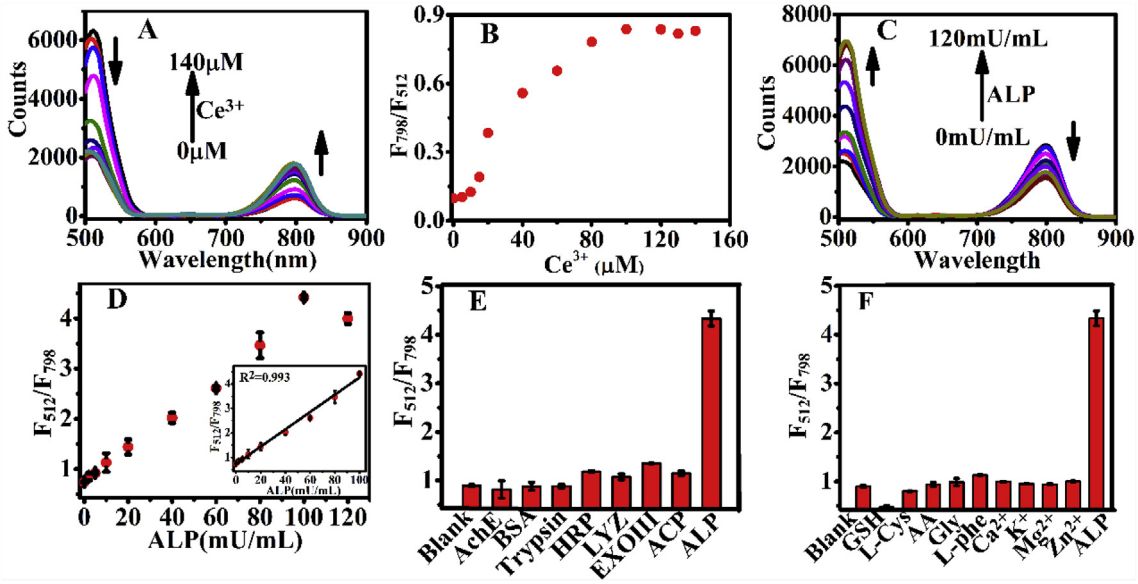

Fig. 3. (A) Fluorescence spectra of the sensing system of 3-MPA-Ag_2S QDs and calcein toward different amounts of Ce^{3+} and (B) the corresponding fluorescence intensity ratio of the system (F_{798}/F_{512}) *vs* the concentration of Ce^{3+}; (C) Fluorescence spectra of the sensing system toward the level of ALP and (D) the corresponding fluorescence intensity ratio of the system (F_{512}/F_{798}) *vs* the level of ALP. Inset in Fig. 3D shows the linear relationship of F_{512}/F_{798} *vs* the level of ALP. Fluorescence sensing system toward various species: (E) AchE, BSA, Trypsin, HRP, LYZ, EXO III, ACP and ALP, the concentration of ALP is 100 mU/mL, and the others are 5 μg/mL; (F) GSH, L-Cys, AA, Gly, L-Phe, Ca^{2+}, K^+, Mg^{2+}, Zn^{2+} and ALP, the concentrations of GSH, L-Cys, AA, Gly, and L-Phe are 0.5 mM, Ca^{2+}, K^+, Mg^{2+}, and Zn^{2+} are 0.01 mM, ALP is 100 mU/mL.

ALP-directed hydrolysis of pNPP results into the generation of orthophosphate. Ce^{3+} ions tend to bind with PO_4^{3-} ($K_{sp} \sim 10^{-24}$) due to the stronger affinity than that of carboxylic group (Qian et al., 2015b; Chen et al., 2018). Therefore, it is reasonable to believe that PO_4^{3-} ions from ALP-directed hydrolysis of pNPP can competitively grasp Ce^{3+} from carboxylic groups of 3-MPA-Ag_2S QDs and calcein and cause the changes of fluorescent intensity.

3.4. Fluorescence detection of ALP

In order to achieve the best performance of the ratiometric fluorescent system, we have optimized the experimental conditions for ALP detection. With the addition of Ce^{3+} into the solution containing 3-MPA-Ag_2S QDs and calcein, the fluorescence intensity at 512 nm is decreased while the signal at 798 nm is enhanced (Fig. 3A). The ratio of fluorescence intensity (F_{798}/F_{512}) is gradually increased along with the increasing concentration of the Ce^{3+} (Fig. 3B). When the concentration of Ce^{3+} is up to 100 μM, the ratio of F_{798}/F_{512} reaches its maximum. Therefore, 100 μM Ce^{3+} is selected for the following experiment. Then, the reaction time for the ALP-directed hydrolysis was investigated in the presence of excessive substrates. As shown in Fig. S5A, the values of F_{512}/F_{798} is increased with the lasting of the reaction time. After reaction for 40 min, the ratio keeps almost constant. Therefore, we choose 40 min as the optimized time for ALP-directed enzymatic reaction. The concentration of pNPP in the system is further optimized. Fig. S5B shows the changes of the ratio F_{512}/F_{798} with the different concentrations of pNPP. It can be observed that F_{512}/F_{798} is increased over the range of 0 to 100 μM of pNPP and then remains stable. Thus, 100 μM of pNPP is selected in the sensing system. In addition, the performance of the sensing system under different pH is also been tested (Fig. S6), and it shows excellent performance at pH 8.0.

Under optimal conditions, the performance of the sensing system for ALP assay has been investigated. The fluorescence intensities at 512 nm gradually increase while the fluorescence intensities at 798 nm decrease with the addition of different concentrations of ALP (0–120 mU/mL) (Fig. 3C). The corresponding fluorescence intensity ratio (F_{512}/F_{798}) is shown in Fig. 3D. The linear relationship is over the range of 2 to 100 mU/mL with the detection limit of 1.28 mU/mL. The performance of this ratiometric fluorescent assay is comparable to other methods for ALP detection, which are listed in Table S1.

The selectivity of the sensing system has been further studied. As shown in Fig. 3E, proteins and enzymes, including AchE, BSA, Trypsin, HRP, LYZ, EXO (III), and ACP, have no interference on the ratio of fluorescence intensity (F_{512}/F_{798}). As for the application in cell imaging, the selectivity for other potential interferences including small biomolecules (i.e., GSH, L-Cys, AA, Gly and L-Phe) and inorganic ions (Ca^{2+}, K^+, Mg^{2+} and Zn^{2+}) are evaluated. Fig. 3F shows that these substances do not affect the detection for ALP as well.

3.5. Application in screening ALP inhibitor

The system can be used to screen ALP inhibitor based on the sensing principle. Levamisole, a common inhibitor for ALP (Kim et al., 2011; Chang et al., 2011), was used as a model in our experiments. As shown in Fig. S7A, with increasing the concentration of levamisole from 0 to 200 μM, the fluorescence intensities of calcein are gradually decreased, while those of 3-MPA-Ag_2S QDs are increased. The inhibition efficiency can be used as a key factor to screening ALP inhibitors. The inhibition efficiency was defined by the following equation:

$$\text{Inhibition efficiency}(\%) = \frac{[(F_{512}/F_{798})_{\text{no inhibitor}} - (F_{512}/F_{798})_{\text{inhibitor}}]}{[(F_{512}/F_{798})_{\text{no inhibitor}} - (F_{512}/F_{798})_0]} \times 100$$

$(F_{512}/F_{798})_{\text{inhibitor}}$ and $(F_{512}/F_{798})_{\text{no inhibitor}}$ refer to the fluorescence intensity ratio of the ALP assay in the presence and absence of inhibitor, and $(F_{512}/F_{798})_0$ refers to the fluorescence intensity ratio of sensing system without ALP and inhibitor. The relationship between inhibition efficiency and the concentration of inhibitor is shown in Fig. S7B. The half maximal inhibitory concentration (IC_{50}) is calculated to be 55.0 μM for levamisole. It is consistent with the reported value (Kim et al., 2011). These results reveal that the ratiometric fluorescent sensing system can be used to screen ALP inhibitors.

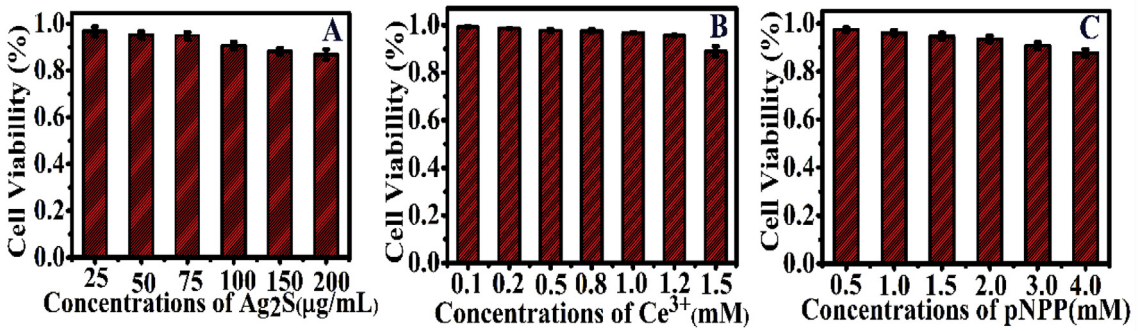

Fig. 4. The viability of Hela cells incubated with different concentrations of (A) 3-MPA-Ag_2S QDs, (B) Ce^{3+} with 75 μg/mL 3-MPA-Ag_2S QDs, and (C) pNPP for 24 h.

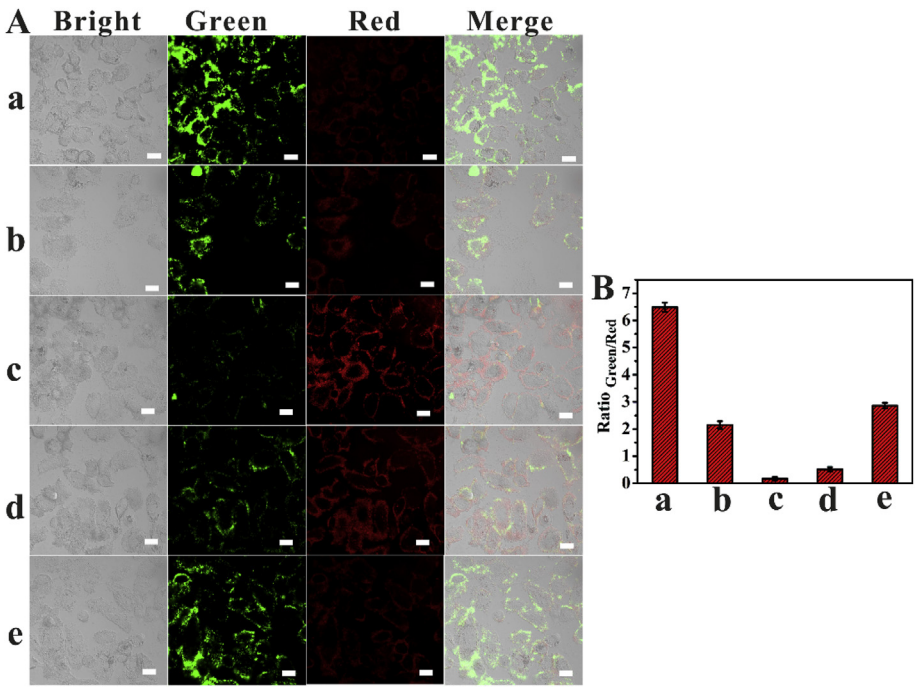

Fig. 5. (A) Confocal images of HeLa cells incubated with (a) 3-MPA-Ag_2S QDs and calcein, (b) 3-MPA-Ag_2S QDs, calcein and 0.5 mM Ce^{3+}, (c) 3-MPA-Ag_2S QDs, calcein and 1 mM Ce^{3+}, (d) 3-MPA-Ag_2S QDs, calcein,1 mM Ce^{3+} and 1 mM pNNP, (e) 3-MPA-Ag_2S QDs, calcein,1 mM Ce^{3+} and 2 mM pNNP. (B) The fluorescence intensity ratio (F_{green}/F_{red}) shown in panels a–e. Scale bar: 20 μm.

3.6. ALP assay in diluted human serum samples

The practicability of the ratiometric fluorescent sensing system for the measurement of ALP is also performed in human serum (10-fold diluted). The results are summarized in Table S2. An acceptable recovery of 100.8–106.2% is obtained and the relative standard deviation is in the range of 2.2 to 7.3%. These data show that the sensing system has a great potential for ALP measurement in real samples.

3.7. Bioimaging of ALP in live cells

The ratiometric assay is further applied in bioimaging intracellular ALP in HeLa cells. Firstly, the cytotoxicity of the system is evaluated by the standard CCK-8 assay. Fig. 4A illustrates that the viability of HeLa cells incubated with 3-MPA-Ag_2S QDs for 24 h with the concentration ranging from 25 to 200 μg/mL, revealing that 3-MPA-Ag_2S QDs are very low cytotoxicity. In addition, the cytotoxicity of 3-MPA-Ag_2S QDs (75 μg/mL) in presence of various concentrations of Ce^{3+} is also investigated (Fig. 4B). The cell viability is not significantly affected by Ce^{3+}, even the concentration of Ce^{3+} is up to 1.5 mM. The effect of pNPP on the viability of HeLa cells is shown in Fig. 4C. It can be observed that the activity of Hela cells is up to 85% even when the concentration of pNPP is as high as 4 mM. These results indicate that the sensing system has good biocompatibility and is suitable for bioimaging ALP in cells.

Inspired by the excellent biocompatibility and selectivity, the ratiometric fluorescent assay for intracellular ALP imaging was further investigated. Firstly, HeLa cells were incubated with 3-MPA-Ag_2S QDs (75 μg/mL) for 12 h, and then incubated with calcein for 30 min. The confocal fluorescent images are shown in Fig. 5A (a). The green channel shows bright green fluorescence of calcein, and the red channel exhibits weak red fluorescence of Ag_2S QDs. After treatment with different concentration of Ce^{3+} for 1 h, the fluorescence signal in green channel is reduced while the red fluorescence is enhanced (Fig. 5A (b) and (c)). With the addition of pNPP into the cell medium, the fluorescence signal in green channel is successfully recovered and the red fluorescence is gradually weakened (Fig. 5A (d) and (e)). It indicates that ALP-directed hydrolysis of pNPP yields PO_4^{3-}, which coordinate with Ce^{3+} and lead to the recovery of fluorescence in green channel and reduction in red channel. Fig. 5B shows the corresponding fluorescence intensity ratio (F_{green}/F_{red}). All of the results indicate that the ratiometric strategy can be employed for ALP bioimaging in living cells.

4. Conclusions

In summary, we have developed a simple, ratiometric fluorescent method for ALP detection based on NIR Ag_2S QDs and calcein with the feature of single-excitation and dual-emission. NIR Ag_2S QDs and

calcein can combine with Ce^{3+} through carboxyl group, which leads to the fluorescence enhancement of Ag_2S QDs by AIE and the fluorescence quenching of calcein by static quenching. PO_4^{3-} released from the hydrolysis of pNPP by ALP can bind with Ce^{3+} competitively and lead to the fluorescence recovery of calcein and the fluorescence attenuation of Ag_2S QDs. Based on these findings, ALP can be easily detected through the fluorescence intensity ratio of calcein at 512 nm and Ag_2S QDs at 798 nm. The detection limit for this strategy is as low as 1.28 mU/mL. Owing to the simplicity, selectivity and sensitivity, the ratiometric fluorescent method has been successfully applied for the screening ALP inhibitor, detection of ALP in human serum and bioimaging of ALP in living cells.

CRediT authorship contribution statement

Meifang Cai: Conceptualization, Funding acquisition, Formal analysis, Writing - original draft, Writing - review & editing. **Caiping Ding:** Conceptualization, Writing - review & editing. **Fangfang Wang:** Formal analysis. **Mingqiang Ye:** Funding acquisition, Writing - review & editing. **Cuiling Zhang:** Conceptualization, Formal analysis, Writing - original draft, Writing - review & editing. **Yuezhong Xian:** Conceptualization, Formal analysis, Writing - review & editing, Writing - original draft.

Acknowledgements

This work was financially supported from National Key R&D Program of China (2018YFF0215404), National Natural Science Foundation of China (21605050, 11727810), Shanghai Natural Science Foundation (18ZR1411300), and the Postdoctoral Science Foundation of China (2018T110367).

Appendix A. Supplementary data

Supplementary data to this article can be found online at https://doi.org/10.1016/j.bios.2019.04.057.

Declaration of interests

☒ The authors declare that they have no known competing financial interests or personal relationships that could have appeared to influence the work reported in this paper.

☒The authors declare the following financial interests/personal relationships which may be considered as potential competing interests:

References

Alonso, A., Sasin, J., Bottini, N., Friedberg, I., Friedberg, I., Osterman, A., Godzik, A., Hunter, T., Dixon, J., Mustelin, T., 2004. Cell 117, 699–711.
Ao, H., Feng, H., Li, K., Zhao, M., Qian, Z., Chen, J., 2018. Sens. Actuators, B 272, 1–7.
Arai, T., Nishijo, T., Matsumae, Y., Zhou, Y., Ino, K., Shiku, H., Matsue, T., 2013. Anal. Chem. 85, 9647–9654.
Berregi, I., Durand, J.S., Casado, J.A., 1999. Talanta 48, 719–728.
Blum, J.S., Li, R.H., Mikos, A.G., Barry, M.A., 2001. J. Cell. Biochem. 80, 532–537.
Chang, L., Mébarek, S., Popowycz, F., Pellet-Rostaing, S., Lemaire, M., Buchet, R., 2011. Bioorg. Med. Chem. Lett 21, 2297–2301.
Chen, C., Zhao, J., Lu, Y., Sun, J., Yang, X., 2018. Anal. Chem. 90, 3505–3511.
Cheng, R., Kong, F., Tong, L., Liu, X., Xu, K., Tang, B., 2018. Anal. Chem. 90, 8116–8122.
Choi, Y., Ho, N.H., Tung, C.H., 2007. Angew. Chem. Int. Ed. 46, 707–709.
Coleman, J.E., 1992. Annu. Rev. Biophys. Biomol. Struct. 21, 441–483.
Colombatto, P., Randone, A., Civitico, G., Monti Gorin, J., Dolci, L., Medaina, N., Oliveri, F., Verrne, G., Marchiaro, G., Pagni, R., Karayiannis, P., Thomas, H.C., Hess, G., Bonino, F., Brunetto, M.R., 1996. J. Viral Hepat. 3, 301–306.
Couttenye, M.M., D'haese, P.C., Van Hoof, V.O., Lemoniatou, E., Goodman, W., Verpooten, G.A., De Broe, M.E., 1996. Nephrol. Dial. Transplant. 11, 1065–1072.
Dai, Z.R., Ge, G.B., Feng, L., Ning, J., Hu, L.H., Jin, Q., Wang, D.D., Lv, X., Dou, T.Y., Cui, J.N., Yang, L., 2015. J. Am. Chem. Soc. 137, 14488–14495.
Deng, J., Yu, P., Yang, L., Mao, L., 2013. Anal. Chem. 85, 2516–2522.
Deng, R., Xie, X., Vendrell, M., Chang, Y.T., Liu, X., 2011. J. Am. Chem. Soc. 133, 20168–20171.
Ding, C., Cao, X., Zhang, C., He, T., Hua, N., Xian, Y., 2017. Nanoscale 9, 14031–14038.
Fan, C., Luo, S., Qi, H., 2016. Luminescence 31, 423–427.
Goggins, S., Naz, C., Marsh, B.J., Frost, C.G., 2015. Chem. Commun. 51, 561–564.
Gui, R., Wan, A., Liu, X., Yuanc, W., Jin, H., 2014. Nanoscale 6, 5467–5473.
Harris, H., 1990. Clin. Chim. Acta 186, 133–150.
Hocaoglu, I., Cizmeciyan, M.N., Erdem, R., Ozen, C., Kurt, A., Sennaroglu, A., Acar, H.Y., 2012. J. Mater. Chem. 22, 14674–14681.
Hu, R., Liu, T., Zhang, X.B., Huan, S.Y., Wu, C., Fu, T., Tan, W., 2014. Anal. Chem. 86, 5009–5016.
Ino, K., Kanno, Y., Arai, T., Inoue, K.Y., Takahashi, Y., Shiku, H., Matsue, T., 2012. Anal. Chem. 84, 7593–7598.
Jiao, H., Chen, J., Li, W., Wang, F., Zhou, H., Li, Y., Yu, C., 2014. ACS Appl. Mater. Interfaces 6, 1979–1985.
Jia, X., Li, J., Wang, E., 2013. Small 9, 3873–3879.
Jin, H., Gui, R., Gong, J., Huang, W., 2017. Biosens. Bioelectron. 92, 378–384.
Julien, S.G., Dubé, N., Hardy, S., Tremblay, M.L., 2011. Nat. Rev. Canc. 11, 35–49.
Kim, T.I., Kim, H., Choi, Y., Kim, Y., 2011. Chem. Commun. 47, 9825–9827.
Lallès, J.P., 2014. Nutr. Rev. 72, 82–94.
Li, N., Li, Y., Han, Y., Pan, W., Zhang, T., Tang, B., 2014. Anal. Chem. 86, 3924–3930.
Li, S.J., Li, C.Y., Li, Y.F., Fei, J., Wu, P., Yang, B., Ou-Yang, J., Nie, S.X., 2017. Anal. Chem. 89, 6854–6860.
Lorente, J.A., Valenzuela, H., Morote, J., Gelabert, A., 1999. Eur. J. Nucl. Med. 26, 625–632.
Lu, L., Wang, M., Mao, Z., Kang, T.S., Chen, X.P., Lu, J.J., Leung, C.H., Ma, D.L., 2016a. Sci. Rep. 6, 22458.
Lu, Z., Wu, J., Liu, W., Zhang, G., Wang, P., 2016b. RSC Adv. 6, 32046–32051.
Ma, J.L., Yin, B.C., Wu, X., Ye, B.C., 2016. Anal. Chem. 88, 9219–9225.
Ooi, K., Shiraki, K., Morishita, Y., Nobori, T., 2007. J. Clin. Lab. Anal. 21, 133–139.
Park, C.S., Ha, T.H., Kim, M., Raja, N., Yun, H., Sung, M.J., Kwon, O.S., Yoon, H., Lee, C.S., 2018. Biosens. Bioelectron. 105, 151–158.
Qian, Z., Chai, L., Tang, C., Huang, Y., Chen, J., Feng, H., 2015b. Anal. Chem. 87, 2966–2973.
Qian, Z., Chai, L., Zhou, Q., Huang, Y., Tang, C., Chen, J., Feng, H., 2015a. Anal. Chem. 87, 7332–7339.
Ruan, C., Wang, W., Gu, B., 2006. Anal. Chem. 78, 3379–3384.
Shi, W., Li, X., Ma, H., 2012. Angew. Chem. Int. Ed. 51, 6432–6435.
Tomita, N., Mori, Y., Kanda, H., Notomi, T., 2008. Nat. Protoc. 3, 877–882.
Tong, Y.J., Yu, L.D., Wu, L.L., Cao, S.P., Liang, R.P., Zhang, L., Xia, X.H., Qiu, J.D., 2018. Chem. Commun. 54, 7487–7490.
Xiang, M.H., Liu, J.W., Li, N., Tang, H., Yu, R., Jiang, J., 2016. Nanoscale 8, 4727–4732.